The effect of limescale on heat transfer in injection molding

Zink Béla, Kovács József Gábor

The effect of limescale on heat transfer in injection molding

Béla Zink[1, a] and József Gábor Kovács[1,b *]

[1] Department of Polymer Engineering, Faculty of Mechanical Engineering, Budapest University of Technology and Economics, Műegyetem rkp. 3., H-1111 Budapest, Hungary

[a] zink@pt.bme.hu, [b] kovacs@pt.bme.hu

* corresponding author

Keywords: injection molding, defects, limescale, precipitation, deposition, conformal cooling, mold cooling design, cooling efficiency

Abstract.

With the development of rapid prototyping technologies, injection mold inserts with conformal cooling systems can be manufactured from metal powder by direct metal laser sintering (DMLS). The conformal cooling channels are placed along the geometry of the injection molded product, thus they can extract more heat, and heat removal is more uniform than in the case of conventional cooling systems. But even the most efficient cooling circuits start to wear out, corrosion and limescale depositions precipitate on the wall of the cooling channel, which impede heat transfer from the mold to the coolant. The effect of the depositions cannot be neglected and the modeling of the impact on heat transfer is difficult. We developed a model to investigate the effect of limescale that formed on the wall of the cooling circuit. The thermal properties of the limescale are required for the simulation, therefore they were measured. We concluded that 2 mm thick limescale impedes heat removal so much that the more efficient conformal cooling system can only extract as much heat as the less efficient conventional system.

1. Introduction

Injection molding has seen rapid progress in the past decades and now it is one of the most important polymer processing technologies. The cooling time of the part is a significant phase of the injection molding cycle. In the case of materials with high processing temperature, large-volume or complicated geometry products, cooling time can be more than half of the whole cycle. With such products a reduction in cooling time considerably improves productivity. One of the best ways to achieve this is to use mold inserts with conformal cooling. As opposed to a conventional cooling system, this system follows the geometry of the product, therefore it can extract more heat and heat extraction is also more uniform, which results in a reduction of cycle time and an improvement in product quality [1]-[7]. Conformal cooling channels are widely

used in the production of plastic parts because of their benefits [8]-[9]. In addition, the use of conformal cooling channels makes it possible to tailor the cooling rate, so in the case of a semicrystalline material, the crystallinity of the injection molded product can be set without fillers [10]-[11].

Mostly water is used to cool the inserts, without any limescale or corrosion inhibition. The thermal conductivity of limescale deposition is two orders of magnitude lower than that of tool steel, which hinders heat transfer from the mold to the coolant. The effect of limescale deposition is more often investigated in the case of heat exchangers, only a few articles focus on injection molds. Pezzin et al. [12] investigated limescale in turbulent flow heat exchangers and concluded that even 2 mm of limescale increases energy consumption by 12%. They approximated the thermal conductivity value of the limescale to be around 2.2 W/(mK), but did not measure its exact value. The effect of limescale and rust in injection molding was analyzed by Novoplan GmbH [13]. The investigations were done with the Moldex 3D injection molding simulation software. They concluded that in the case of their box-shaped product 1 mm of rust increases mold surface temperature by 20 °C and warpage by 0.4 mm. 1 mm of limescale has a bigger impact on temperature and warpage; it doubles the values caused by rust. Furthermore, the efficiency of the cooling circuits drops by 6%. The authors did not specify the thermal conductivity of the depositions in their work and did not give information about the method of measuring thermal conductivity.

Injection molding simulations are used to make proper cooling layouts and it is even more important to use computer calculations for conformal cooling systems. The accuracy of the results is greatly influenced by the precision of modeling, boundary conditions and the calculation algorithms.

More and more articles focus on the development of injection molding simulations to get faster and more accurate results. Zhang et al. [14] developed a novel boundary element method based cooling simulation method for steady-state cooling. The analytical solution of the part temperature was introduced into the boundary element method, so the RAM size required for the calculations was reduced on average by 93% and calculation time was shortened by one order of magnitude. Liu and Gehde [15] analyzed the influence of the heat transfer coefficient between the polymer and the cavity wall on cooling and crystallinity. They found that melt temperature and surface roughness have an important role in determining the HTC. A difference between the frozen percentages calculated by the observed and preset HTC values were reported, and the HTC also influenced relative crystallinity. Kovács et al. [16] determined the influence of the thermal parameters of the prototype mold insert based on the measured temperature results. It was concluded that numerical calculations can be used to determine

thermal and other parameters of rapid-tooled mold inserts, but the calculated results are only approximations, because the numerical algorithm cannot handle the temperature and pressure dependence of the thermal properties of prototype molds. Urquhart and Brown [17] investigated the effects of uncertainty in heat transfer data using numerical analysis. They concluded that uncertainties in the thermal conductivity of the mold and the heat transfer coefficient between the mold and melt only have a minor effect on the time to reach ejection temperature compared to the thermal conductivity of the polymer melt. Only a change of about 10% in mold thermal conductivity can affect the temperature results significantly. The effect of the heat transfer coefficient is even smaller, a significant change in the results can only be observed in the case of thin-walled parts (maximum thickness 0.5 mm) and with a change of two orders of magnitude in the heat transfer coefficient.

2. Heat transfer equations

Nomenclature			
A	cross section, m^2	α	heat transfer coefficient, $Wm^{-2}K^{-1}$
g	gravitational acceleration, ms^{-2}	β	polymer expansivity, K^{-1}
p	pressure, Pa	δ	thickness, m
c_p	specific heat, $Jkg^{-1}K^{-1}$	ε	emissivity, -
t	time, s	ρ	density, kgm^{-3}
ΔT	temperature difference, °C	λ	thermal conductivity, $Wm^{-1}K^{-1}$
v	velocity, ms^{-1}	σ_0	Stefan-Boltzmann constant, $Wm^{-2}K^{-4}$
R	heat resistance, KW^{-1}	R_α	heat resistance caused by heat transfer, KW^{-1}
R_λ	heat resistance caused by conduction, KW^{-1}	r_1	inner diameter of the limescale deposition, m
$\lambda_{limescale}$	thermal conductivity of limescale, $Wm^{-1}K^{-1}$	r_2	outer diameter of the limescale deposition, m
$\alpha_{coolant\text{-}limescale}$	heat transfer coefficient between coolant and limescale, $Wm^{-2}K^{-1}$	L	length of the limescale deposition, m

From a thermal aspect, injection molding starts with the injection phase, where the melt is injected into the tempered cavity at a high speed until the cavity is fully filled. The melt starts to transmit energy to the mold right after it touches the wall of the mold. In the upcoming packing phase some more melt is forced into the cavity, so more heat is taken into the mold. The pressure drops during the cooling stage until it reaches atmospheric pressure, and because of volumetric shrinkage, air gaps are formed at several places between the cavity wall and the injection molded part. The intensity of heat removal is the highest in the injection phase, because cavity pressure and the temperature difference between the melt near the wall and the

cavity wall are the highest. The calculation of melt flow and temperature distribution can be executed by Navier-Stoke's momentum (1), continuity (2) and energy (3) conservation equations [18], [19]:

$$\varrho \cdot \left(\frac{\partial \boldsymbol{v}}{\partial t} + \boldsymbol{v} \cdot \nabla \boldsymbol{v}\right) = -\nabla \boldsymbol{p} + \nabla\left(\eta \cdot (\nabla \boldsymbol{v} + (\nabla \boldsymbol{v})^T)\right) - \frac{2}{3}\eta \cdot \nabla(\nabla \boldsymbol{v}) + \varrho \cdot \boldsymbol{g}, \quad (1)$$

$$\frac{\partial \varrho}{\partial t} + \nabla(\varrho \boldsymbol{v}) = 0, \quad (2)$$

$$\varrho \cdot c_p \cdot \left(\frac{\partial \boldsymbol{T}}{\partial t} + \boldsymbol{v} \cdot \nabla \mathbf{T}\right) = \nabla(\lambda \cdot \nabla \mathbf{T}) + \boldsymbol{T} \cdot \beta \cdot \left(\frac{\partial \boldsymbol{p}}{\partial t} + \boldsymbol{v} \cdot \nabla \mathbf{T}\right), \quad (3)$$

where,

$$\beta = -\frac{1}{\varrho}\frac{\partial \boldsymbol{p}}{\partial \boldsymbol{T}}. \quad (4)$$

The heat from inside the cavity is removed by conduction, radiation and heat transfer (Fig. 1.). This heat transfer from the melt to the mold, clamping unit and the atmosphere can be decomposed with the following equations [20]:

$$\dot{Q} = \int_0^{t_{cycle}} \sigma_0 \cdot \varepsilon \cdot \mathrm{A} \cdot \Delta \mathrm{T}^4 \cdot dt, \quad (5)$$

$$\dot{Q} = \int_0^{t_{cycle}} \frac{\lambda}{\delta} \cdot \mathrm{A} \cdot \Delta \mathrm{T} \cdot dt, \quad (6)$$

$$\dot{Q} = \int_0^{t_{cycle}} \alpha \cdot \mathrm{A} \cdot \Delta \mathrm{T} \cdot dt. \quad (7)$$

The heat removal of the cooling channels is blocked by the limescale deposition formed in the cooling channels. The limescale deposition consists mainly of $CaCO_3$ and $MgCO_3$, and precipitates from the cooling water. Carbonates dissolve poorly in water, but the CO_2 physically dissolved in the water converts them into hydrogen carbonate, which dissolves better [21]:

$$CaCO_3 + CO_2 + H_2O \rightleftharpoons Ca(HCO_3)_2, \quad (8)$$

$$MgCO_3 + CO_2 + H_2O \rightleftharpoons Mg(HCO_3)_2. \quad (9)$$

As the concentration of carbon dioxide decreases, the equilibrium in these reactions shifts to the left and the carbonates precipitate, and limescale is formed. This layer of limescale inhibits heat removal between the mold insert and the coolant. Eq. (9) describes the heat resistance caused by the limescale [20]:

$$R = R_\alpha + R_\lambda = \frac{1}{2 \cdot L \cdot r_1 \cdot \pi \cdot \alpha_{coolant-limescale}} + \frac{ln\left(\frac{r_2}{r_1}\right)}{2 \cdot L \cdot \pi \cdot \lambda_{limescale}}. \quad (10)$$

3. Experimental

The purpose of the experiments was to investigate the effect of limescale on different cooling circuits and mold materials. Three mold inserts were investigated with two different cooling circuits and mold materials.

Mold materials Three mold materials (Table 1) were used in the experiments: MaragingSteel MS1 (MS1), Böhler 1.2311 (P20) and Ampcoloy 88.

	1.2311	MS1	Ampcoloy 88
Density (kg/m^3)	**7800**	**8100**	**8750**
Tensile strength (MPa)	**1020**	**1950**	**890**
Yield point (MPa)	**900**	**1900**	**680**
Young's modulus (GPa)	**250**	**180**	**130**
Thermal conductivity coefficient (W/(mK))	**29**	**20**	**230**
Specific heat capacity (J/(kgK))	**460**	**450**	**420**

Table 1. The main characteristics of the materials used in the simulations

Mold design Two different mold inserts were modeled in a two-cavity mold block for the cooling simulations (Fig. 2/a). Our reference was the setup most often used in industry: 1.2311 steel mold insert with a conventional cooling geometry (P20 insert) (Fig. 2/b). The same conventional cooling system was used with Ampcoloy 88 highly alloyed copper for the second insert (Ampcoloy insert). The third setup was the MS1 steel mold insert with a conformal cooling system, which can be made by Direct Metal Laser Sintering (DMLS insert) (Fig. 2/c).

The thermal parameters of limescale

Specific heat (c_p) was measured by DSC (TA Instruments Q2000), density (ρ) by means of Archimedes' principle (Ohaus explorer scale) and thermal conductivity (λ) with a heat flow conductivity meter (Fig. 3.). The thermal properties of limescale depend on its composition, which depends on the cooling water itself, therefore, six different limescale samples were measured. The measurement of conductivity is based on the comparative longitudinal heat flow method. The sample with unknown conductivity is compressed between the known reference samples and as a temperature difference is created between the two sides of the unit, a heat flux passes through the measurement unit. The reference cylinders consist of C10 steel (55 W/(mK)) with a diameter of 30 mm and a length of 30 mm. The limescale samples were grinded and pressed between the reference cylinders with a pressure of 60, 120, 180, 250, 300, 425, and 550 bar. From the calculated conductivity values for each pressure level the heat conductivity of a dense limescale sample can be obtained by fitting a sigmoid curve on the calculated conductivity values. Thermal grease was applied on the contact surface of the pressed sample and the reference cylinders to decrease heat resistance. Three thermocouples were inserted in each cylinder to record temperature; one 3 mm below the top, one in the middle and one 3 mm above the bottom ($T_{m1,2,3,4,5,6}$/Fig. 3.).

The temperatures were registered with an Ahlborn Almemo 8990-6-V5 data acquisition module, whose resolution is 0.1°C. The apparatus was clamped and the temperature difference maintained with a hot press on the Collin Teach-Line Platen Press 200E. The assembled unit was insulated with polyurethane foam to minimize heat loss. When the steady state is reached, the temperature slope is linear along the reference sample and the specimen thickness, so the surface temperatures ($T_{1,2,3,4}$/Fig. 3.) can be calculated by extrapolation from the measured temperatures. From the thermal conductivity of steel and the temperature difference between the surfaces, the heat flux of the hot and cold sides can be calculated with Fourier's law. From the average of the heat fluxes the thermal conductivity coefficient of the samples ($\lambda(p)$) can be calculated with Equation (10).

$$\lambda(\mathrm{p}) = \lambda_{\mathrm{r}} \frac{\mathrm{A_r} \cdot \frac{1}{\mathrm{n}} \sum_{\mathrm{i}=1}^{\mathrm{n}} \frac{\Delta \mathrm{T_i}}{\mathrm{x_i}}}{\frac{\mathrm{A_c}}{\mathrm{x_c}} \cdot \Delta \mathrm{T_c}}, \tag{10}$$

where λ_r is the thermal conductivity coefficient, A_r is the cross-section of the reference steel cylinder, x_i is the distance between the sensors, ΔT_i is the temperature differences measured by the sensors, A_c and x_c are the cross-section and the thickness of the sample, and ΔT_c is the temperature drop on the sample. The cold side was 50°C and the hot side was 80°C, therefore the average temperature was 65°C. This large difference in temperature was required to achieve a more precise result, because the thermal conductivity of the reference sample is significantly higher than the thermal conductivity of the limescale sample. We fitted a sigmoid curve (Equation (11)) to the measured values of pressure-dependent thermal conductivity to determine the theoretical maximum thermal conductivity of the compacted limescale.

$$\lambda(\mathrm{p}) = \lambda_{\infty} \frac{1 - \mathrm{e}^{-\mathrm{n} \cdot \mathrm{p}^{\mathrm{m}}}}{1 + \mathrm{e}^{-\mathrm{n} \cdot \mathrm{p}^{\mathrm{m}}}} \; (0 \le \mathrm{p} \le \infty), \tag{11}$$

where n and m are data fitting parameters, and λ_∞ is the thermal conductivity coefficient at infinite pressure (p), which corresponds to the thermal conductivity coefficient of the bulk material. As we expected, the calculated conductivity values vary in a wide range (Fig. 4.). The fitting of the sigmoid curves is precise; the average of the fitting errors is only 0.14±0.04 W/(mK). The average of the conductivity values is λ=1.37±0.43 W/(mK), which is a bit lower than the values mentioned in some articles (1.7-2.3 W/(mK)).

Specific heat was measured in the most common cooling temperature range, 0-120°C, with a heat-cool-heat protocol with a heating and cooling speed of 2°C/min. The specific heat of the limescale depends on the temperature, varying between 700 J/(kgK) and 900 J/(kgK) in the investigated temperature range (Fig. 5.). An average specific heat of about 800 J/(kgK) was

used for the calculations. The density of the limescale was only measured in the case of block-shaped limescale specimens; the average density was 1,20±0,064 g/cm^3.

Simulation

We made the simulations with the Autodesk Simulation Moldflow Insight 2016 and CFD 2016 programs, using ABS (BASF, Terluran GP35). Four-node tetrahedral elements were used in the entire model including parts, mold inserts and cooling circuits (Fig. 6.).

Four-node tetrahedral elements make it possible to consider heat conduction in all directions and calculate the temperature in all nodes. The limescale deposition was modeled into the CAD model and the entire model was meshed in Moldflow. Limescale depositions with a thickness of 0.25 mm, 0.5 mm, 1 mm and 2 mm were investigated, and the averaged physical properties (λ= 1.37 W/(mK), cp= 800 J/(kgK), ρ= 1.2 g/cm^3) were used for the thermal calculations. Eight simulation models were used in the study, because two types of inserts were modeled in each simulation model and every limescale thickness has to have its own model. Global element size was set to 1.6 mm, but mesh size was decreased to 0.6 mm in areas where it was required by the complex geometry, for example the gate and the cooling channels. 6 layers of elements were used in the thickness direction for every component, including the limescale depositions. The number of elements was around 6 million for every model. Cool FEM was used for the thermal analysis, which provides options to investigate the transient stage of the mold. We used a conduction solver to calculate heat flux. Perfect clamping was assumed, therefore mold block conductance was set to the default 30000 W/m^{2}K) (Table 2).

Melt temperature (°C)	**240**
Ejection temperature (°C)	**120**
Ambient temperature (°C)	**25**
Mold surface temperature (°C)	**40**
Cooling time (s)	**18**
Initial mold temperature (°C)	**40**
Mold block conductance (W/(m^{2}K))	**30000**

Table 2. The parameters used in the simulation study

4. Results and discussion

The cycle-averaged temperature results of the mold-circuit interface were evaluated along the main edge of the moving half mold insert (Fig. 7/b.). The zero point of the edge is on the outer side of the insert. The main edge of the insert is the most difficult to cool because of its geometry. The cooling circuits cannot be moved close enough to the surface, and the main edge distracts heat from two surfaces of the specimen (Fig. 7/a).

In the case of limescale-free cooling circuits, the P20 insert has the worst heat removal (

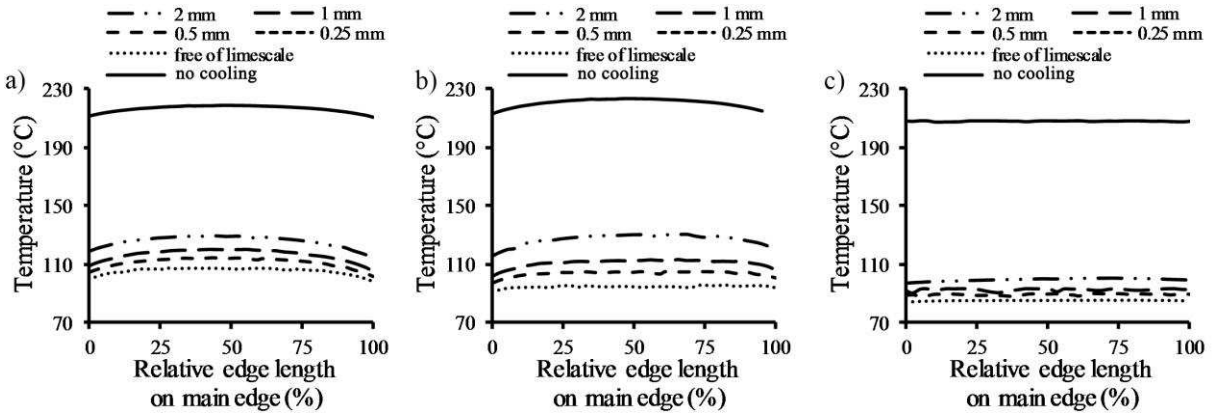

Fig. 8/a), while the Ampcoloy insert is the best (

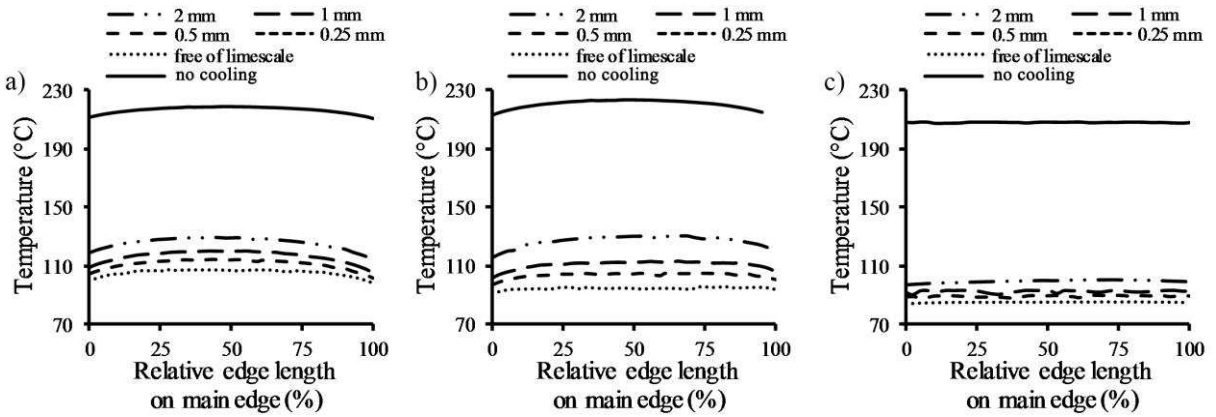

Fig. 8/c), The DMLS mold insert is between the two in terms of heat removal (

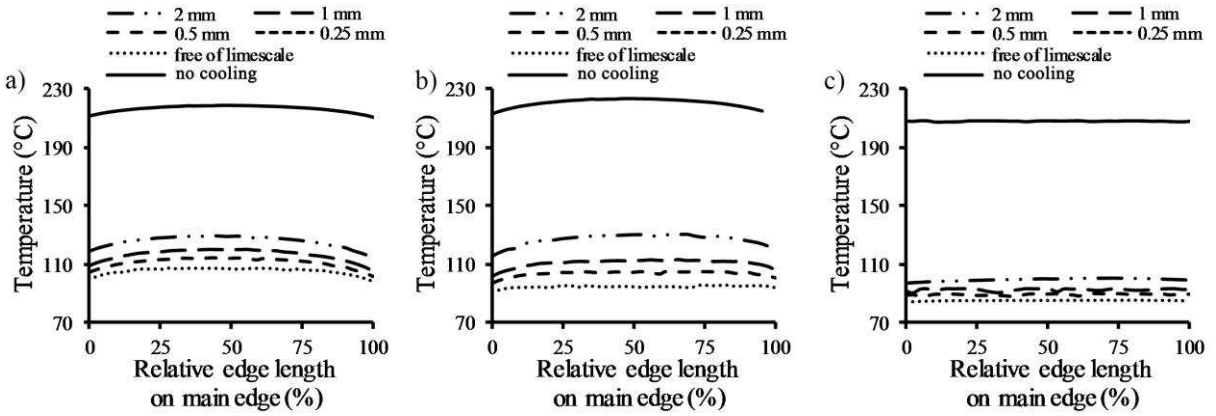

Fig. 8/b). In the case of all mold inserts, surface temperature rose as the thickness of limescale increased. When the limescale layer was 2 mm thick, the temperature distribution of the DMLS mold insert with the better cooling efficiency was almost exactly the same as in the case of the P20 insert. This suggests that in the case of the DMLS mold insert, the 2 mm limescale layer decreases heat removal in the direction of the cooling circuits to the level of the P20 insert, thus the complex-shaped cooling channels can only extract as much heat as the single, drilled channel of the P20 insert. Therefore the amount of heat conducted through the DMLS inserts and from the cavity to the adjacent mold block increases. If there are no cooling channels in the insert, the maximal temperature for the DMLS and P20 inserts is around 220 °C. The

temperature of the DMLS insert is slightly higher than the P20 insert because the thermal conductivity of MS1 is a bit lower. In the case of the Ampcoloy insert, the effect of limescale is about half the above, a 2 mm deposition increases the surface temperature of the mold insert by about 18%. This can be attributed to the fact that due to the high thermal conductivity coefficient of the Ampcoloy insert, heat can be removed from the critical corner even if the efficiency of the cooling circuit decreases drastically.

The specific heat of the examined limescale samples is temperature-dependent and their thermal conductivities vary between 0.56-1.74 W/mK, therefore we analyzed the effect of the thermal parameters of limescale on temperature. The 1 mm limescale deposit model was used with Ampcoloy and DMLS mold inserts. Thermal conductivity and specific heat were modified (λ= 0.56, 1.37, 1.74 W/(mK), c_p= 700, 900 J/(kgK)), while density was not changed (1.2 g/cm^3).

Based on the results (Fig 9), it can be stated that the effect of specific heat on the calculation results in the interval of the measured values (700-900 J/kgK) is negligible, which was proved with linear regression (Fig 9/a). The effect of the thermal conductivity coefficient was evaluated in the middle of the main edge of the insert, where the temperature maximum can be found. In the investigated thermal conductivity coefficient interval the thermal conductivity of the limescale deposit greatly influences the calculated results in the case of the DMLS insert (Fig 9/b), and as can be expected, lower thermal conductivity results in higher temperatures. The increase in temperature is not directly proportional to the thickness in mold inserts; the λ=1.37 W/(mK) limescale layer only increases temperature by 2-3 °C compared to λ=1.74 W/(mK). On the other hand, a limescale layer of λ=0.56 W/(mK) results in a temperature increase of nearly 15°C, therefore it can be stated that in the case of steel mold inserts with conformal cooling, both the thickness and the composition of the limescale deposit have a pronounced effect on cooling efficiency. In the case of copper mold inserts, the change in temperature is smaller and temperature change is close to linear as a function of thermal conductivity.

5. Summary

We investigated the effect of limescale deposition on cooling efficiency with numerical calculations. We created three models in a CAD system for the experiments. We added the limescale deposit into the cooling channels and imported the whole model into Moldflow 2016 and meshed it. The thermal properties of the limescale are influenced by its composition, therefore they were measured on six different samples. The cycle-averaged temperature results of the mold-circuit interface show a minor increase for the P20 insert, which has a conventional cooling system. A 2 mm thick limescale deposition hinders heat extraction of the conformal

cooling channel of the DMLS insert, therefore the temperature distribution along the main edge of the DMLS insert is equal to that of the temperature distribution of the P20 insert. In the case of the Ampcoloy 88 insert, the effect of limescale is minor, which can be explained by the heat extraction process: in the case of the DMLS insert, the heat is extracted by the cooling channels, as opposed to the Ampcoloy insert, where heat is extracted not only by the cooling channels, but also by the insert material itself, which has a thermal conductivity coefficient one order of magnitude higher. The specific heat of the limescale is temperature-dependent, but in the temperature range of the cooling water its effect on temperature distribution can be neglected. In addition to the thickness of limescale, heat extraction is mostly affected by the thermal conductivity of the limescale, which depends on the water used for cooling. The surface temperature distribution of the DMLS insert depends more on the thermal conductivity of the deposit than the temperature-distribution of the Ampcoloy insert does. In the case of the DMLS insert, the reduction in cooling efficiency is not directly proportional to the heat conductivity increase of the deposition; a limescale deposition with a thermal conductivity below 1.37 W/mK produces a rate of increase in surface temperature higher than a layer of limescale above 1.37 W/mK.

6. Acknowledgements

The authors wish to thank the Autodesk Inc for the simulation software, and especially Franco Costa, Senior Research Leader.

References

[1] W. Michaeli, M. Schönfeld, Komplexe Formteile kühlen, Kunststoffe, 8 (2006) 37-41.

[2] Y. Zhang, Z. Huang, H. Zhou, D. Li, A rapid BEM-based method for cooling simulation of injection molding, Engineering Analysis with Boundary Elements 52 (2015) 110–119 DOI: 10.1016/j.enganabound.2014.11.020

[3] J. Meckley, R. Edwards, A study on the design and effectiveness of conformal cooling channels in rapid tooling inserts, Technology Interface Journal 10 (2009) 1-28.

[4] A. Coremans, M. Kauf, P. Hoffmann, Laser assisted rapid tooling of molds and dies, Proceedings of the 5th European Conference on Rapid Prototyping and Manufacturing Helsinki Finland (1996) 195-210.

[5] L-E. Rännar, A. Glad, C-G. Gustafson, Efficient cooling with tool inserts manufactured by electron beam melting, Rapid Prototyping Journal 13 (2007) 128-135. DOI: 10.1108/13552540710750870

[6] E. Vojnová, The benefits of a conforming cooling systems the molds in injection moulding process, Procedia Engineering 149 (2016) 535–543.

[7] K. Eiamsa-ard, K. Wannissorn, Conformal bubbler cooling for molds by metal deposition process, Computer-Aided Design 69 (2015) 126–133.

[8] B. He, L. Ying, X. Li, P. Hu, Optimal design of longitudinal conformal cooling channels in hot stamping tools, Applied Thermal Engineering 106 (2016) 1176–1189.

[9] R. Hölker, M. Haase, N. B. Khalifa, A. E. Tekkaya, Hot extrusion dies with conformal cooling channels produced by additive manufacturing, Materials Today: Proceedings 2 (2015) 4838 – 4846.

[10] A. Kmetty, T. Tabi, J. G. Kovacs, T. Barany, Development and characterisation of injection moulded, all-polypropylene composites, Express Polymer Letters 7 (2013) 134-145. DOI: 10.3144/expresspolymlett.2013.13

[11] A. Makhlouf, H. Satha, D. Frihi, S. Gherib, R. Seguela, Optimization of the crystallinity of polypropylene/submicronic-talc composites: The role of filler ratio and cooling rate, eXPRESS Polymer Letters 10 (2016) 237–247. ISSN: 1788-618X

[12] A. Pezzin, M. Giansetti, A. Ferri, Influence of Limescale on Heating Elements Efficiency, COMSOL Conference, Rotterdam (2013)

[13] Novoplan GmbH, Rostfreie Temperierung senkt die Stückkosten, Kunststoffe 7 (2007) 60-61.

[14] Y. Zhang, Z. Huang, H. Zhou, D. Li, A rapid BEM-based method for cooling simulation of injection molding, Engineering Analysis with Boundary Elements 52 (2015) 110–119. DOI:10.1016/j.enganabound.2014.11.020

[15] Y. Liu, M. Gehde, Evaluation of heat transfer coefficient between polymer and cavity wall for improving cooling and crystallinity results in injection molding simulation, Applied Thermal Engineering 80 (2015) 238-246.

[16] J. G. Kovacs, F. Szabo, N. K. Kovacs, A. Suplicz, B. Zink, T. Tabi, H. Hargitai, Thermal simulations and measurements for rapid tool inserts in injection molding applications, Applied Thermal Engineering 85 (2015) 44-51.

[17] J. M. Urquhart, C. S. Brown, The effect of uncertainty in heat transfer data on the simulation of polymer processing, NPL Report DEPC-MPR 001 (2004) ISSN: 1744-0270

[18] H. Hassan, N. Regnier, C. Le Bot, G. Defaye, 3D study of cooling system effect on the heat transfer during polymer injection molding, International Journal of Thermal Sciences 49 (2010) 161-169.

[19] Y. Liu, M. Gehde, Evaluation of heat transfer coefficient between polymer and cavity wall for improving cooling and crystallinity results in injection molding simulation, Applied Thermal Engineering 80 (2015) 238-246.

[20] Y. Liu, M. Gehde, Effects of surface roughness and processing parameters on heat transfer coefficient between polymer and cavity wall during injection molding, The International Journal of Advanced Manufacturing Technology 84 (5) (2016) 1325–1333.

[21] E. Stamatakis, A. Stubos, J. Muller, Scale prediction in liquid flow through porous media: A geochemical model for the simulation of CaCO3 deposition at the near-well region, Journal of Geochemical Exploration 108 (2011) 115-125.

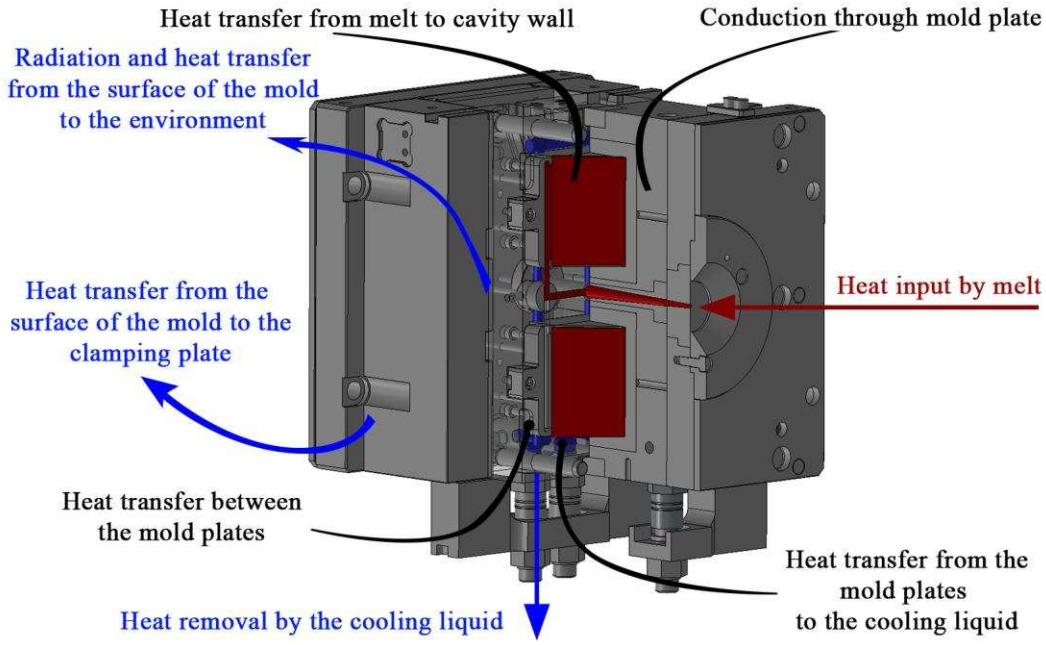

Fig. 1. Total heat flow in the mold

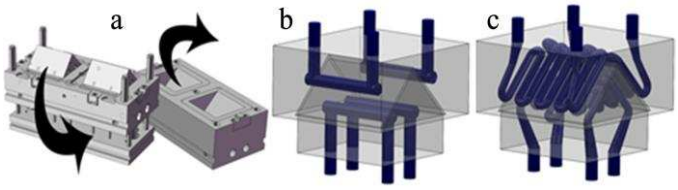

Fig. 2. The injection mold block used in the simulations (a) the Conventional (b) and Conformal (d) cooling systems of the inserts

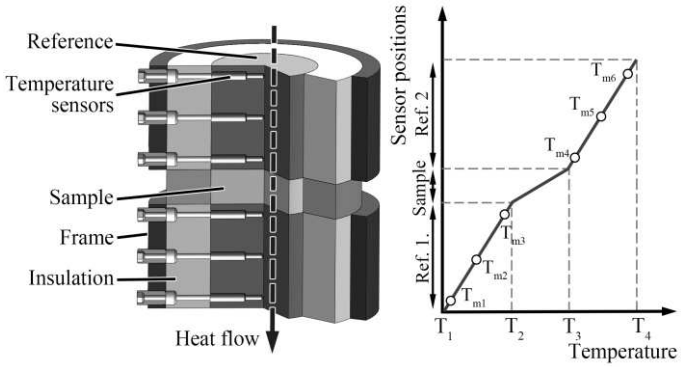

Fig. 3. The buildup and the temperature distribution of the thermal conductivity meter

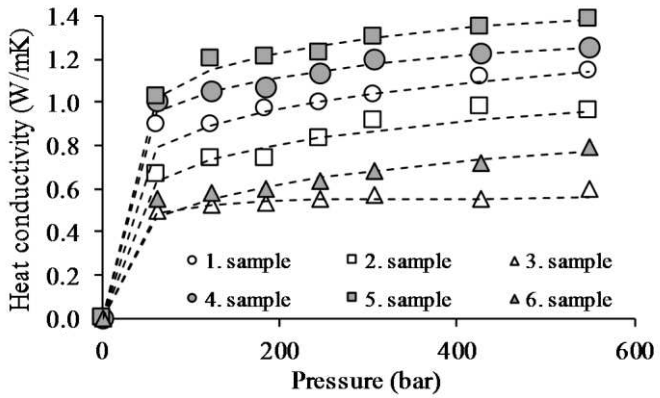

Fig. 4. The calculated conductivity values and the fitted sigmoid curves

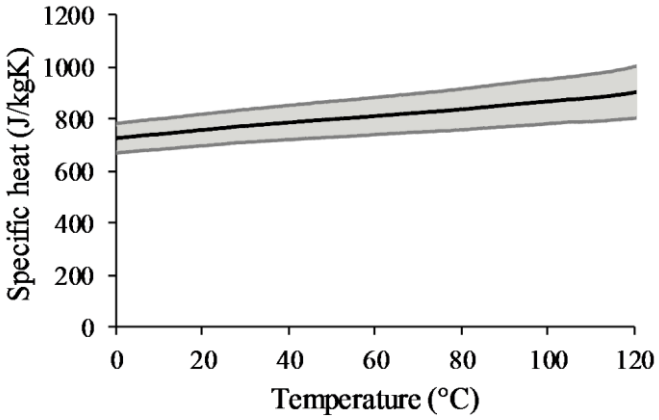

Fig. 5. The specific heat and standard deviation as a function of temperature

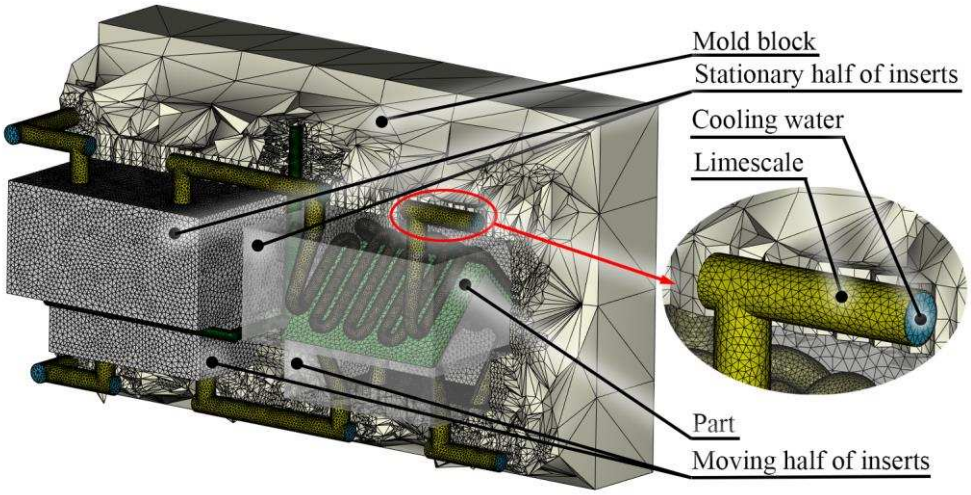

Fig. 6. Simulation model, with limescale in the cooling channels magnified

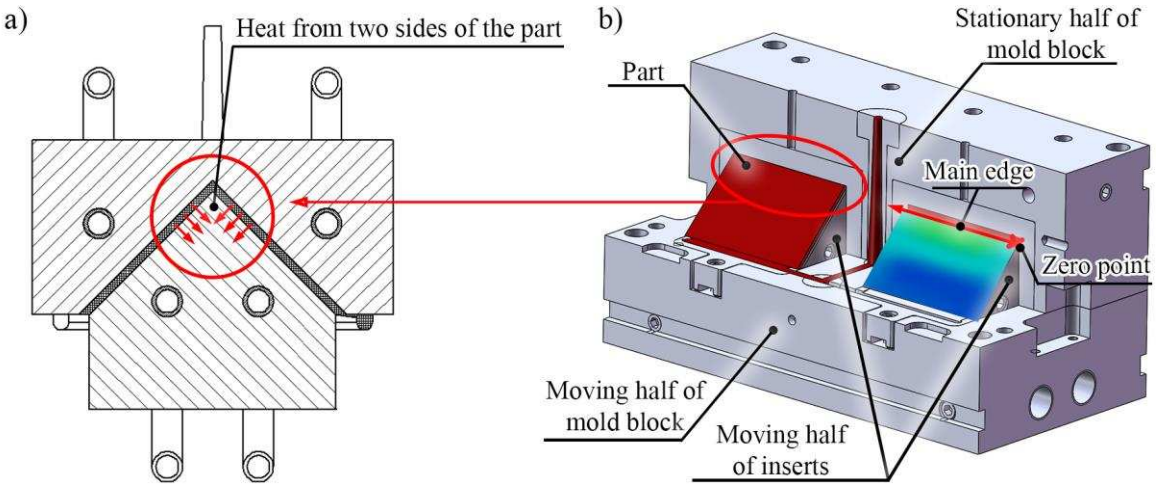

Fig. 7. The heat energy transmitted to the moving inserts (a) and the main edge used for the evaluation of the temperature results (b)

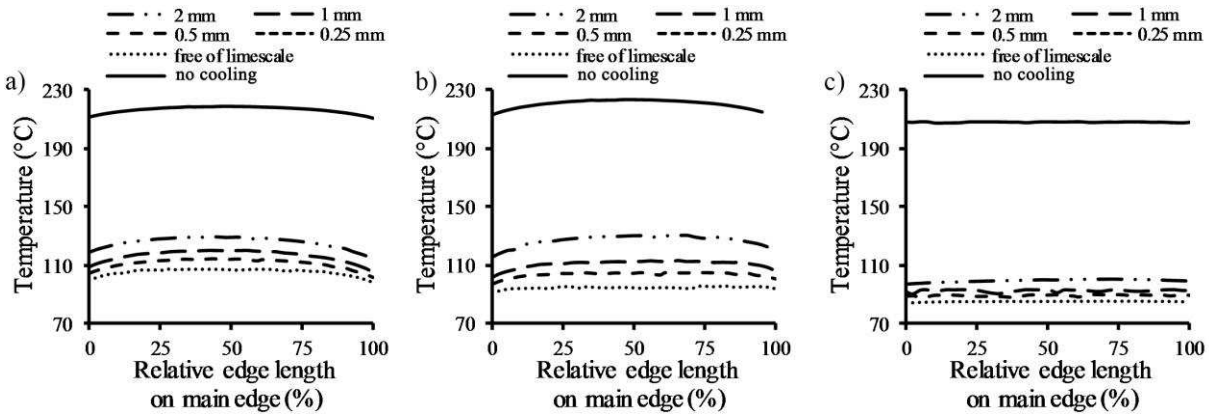

Fig. 8. The effect of limescale layers of various thicknesses on heat distribution along the main edge of P20 (a), DMLS (b) and Ampcoloy (c) mold inserts

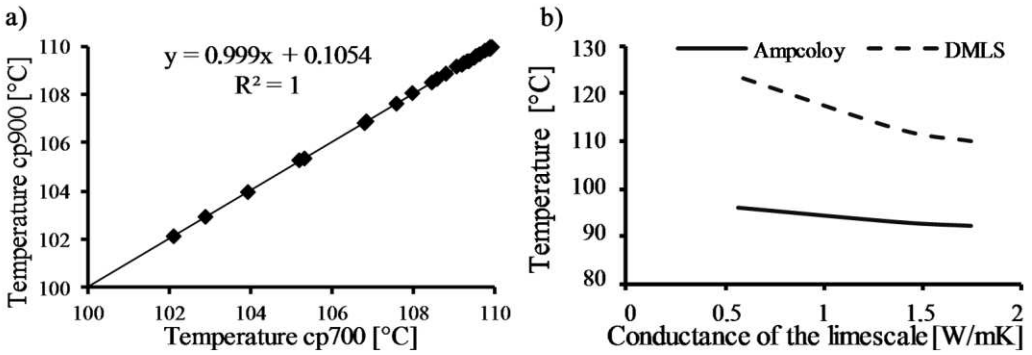

Fig 9. The effect of modifying specific heat (a) and thermal conductivity (b) on the surface temperature of the mold insert